Ecosystems
DOI: 10.1007/s10021-016-0038-3

ECOSYSTEMS

Modeled Effects of Climate Change and Plant Invasion on Watershed Function Across a Steep Tropical Rainfall Gradient

Ayron M. Strauch,[1]* Christian P. Giardina,[2] Richard A. MacKenzie,[2] Chris Heider,[3] Tom W. Giambelluca,[4] Ed Salminen,[5] and Gregory L. Bruland[6]

[1]*Department of Natural Resources and Environmental Management, University of Hawai'i at Mānoa, 1910 East-West Road, Sherman 101, Honolulu, Hawai'i 96822, USA;* [2]*USDA Forest Service Pacific Southwest Station, 60 Nowelo Street, Hilo, Hawai'i 96720, USA;* [3]*Watershed Professionals Network, B.O. Box 1641, Philomath, Oregon 97370, USA;* [4]*Department of Geography, University of Hawai'i at Mānoa, 2424 Maile Way, 445 Saunders Hall, Honolulu, Hawai'i 96822, USA;* [5]*Watershed Professionals Network, P.O. Box 8, Mount Hood, Oregon 97041, USA;* [6]*Department of Biology and Natural Resources, Principia College, 1 Maybeck Place, Elsah, Illinois 62028, USA*

ABSTRACT

Climate change is anticipated to affect freshwater resources, but baseline data on the functioning of tropical watersheds is lacking, limiting efforts that seek to predict how watershed processes, water supply, and streamflow respond to anticipated changes in climate and vegetation change, and to management. To address this data gap, we applied the distributed hydrology soil vegetation model (DHSVM) across 88 watersheds spanning a highly constrained, 4500 mm mean annual rainfall (MAR) gradient on Hawai'i Island to quantify stream flow at 3-h time-steps for eight years in response to the independent and interactive effects of (1) large observed decrease in MAR; (2) projected warming and altered precipitation; and (3) four scenarios of forest invasion by the high water-demanding non-native tree species *Psidium cattleianum*. The model captured 62% of variability in measured flow at daily time scales, 95% at monthly time scales, and 98% at annual time scales. We found that low DHSVM modeled flow (Q_{90}) and storm flow (Q_{10}) responses to observed declines in rainfall dwarfed those of projected temperature increase or invasion, with flow decline positively correlated with MAR. As a percentage of streamflow, temperature and invasion reductions were negatively correlated with MAR. By comparison, warming alone had little effect on Q_{90} or Q_{10}, but both decreased with increasing *P. cattleianum* cover, and projected effects of declining MAR were accentuated when combined with *P. cattleianum* and warming. Restoration mitigated some effects of climate warming by increasing stream base flows, with the relative effects of restoration being larger in drier versus wetter watersheds. We conclude that potential changes in climate in tropical environments are likely to exert significant effects on streamflow, but managing vegetation can provide mitigating benefits.

Received 5 June 2015; accepted 29 July 2016;

Electronic supplementary material: The online version of this article (doi:10.1007/s10021-016-0038-3) contains supplementary material, which is available to authorized users.

Author contributions CPG, CH, and RAM conceived of or designed study. CH, ES, and CPG performed research. AMS analyzed data. CH, ES, and TWG contributed methods or models. AMS, RAM, CPG, TWG, CH, ES, and GLB wrote or provided comments to the paper.

*Corresponding author; e-mail: astrauch@hawaii.edu

Published online: 23 September 2016

Key words: climate change; Hawai'i; streamflow; *Psidium cattleianum*; invasive species; DHSVM; restoration.

Introduction

Climate warming and changes to the magnitude and frequency of rainfall events (IPCC 2013; Muller and others 2011), the spread of non-native and invasive plants that increase stand water use, and their interactions are projected to affect the Earth's water resources, with resulting declines in the supply of freshwater for human and natural systems (Asner and others 2008; Cavaleri and others 2014; Chapin III and others 2010; Milly and others 2005). Despite progress in conserving forest cover in tropical watersheds, these effects may be especially large in the humid tropics (Foster 2001; Wohl and others 2012), and where climate-related threats will continue to increase in severity, with anticipated affects to industry, agriculture, tourism, human health, and ecosystem function (Chapin III and others 2010; IPCC 2013; Milly and others 2005). While extensive efforts have been directed at forecasting rainfall and temperature patterns in the tropics, relatively little is known about how these effects will translate into watershed function (Wohl and others 2012).

Effects of climate change on the water cycle are complex because altered temperature and rainfall affect numerous processes operating at individual leaf to watershed scales, which in turn affect the timing and availability of freshwater resources. For example, warming affects transpiration and water use by vegetation, and temperature and precipitation changes are accompanied by changes in relative humidity, solar radiation, transpiration, evaporation from the canopy and soil surfaces, groundwater recharge, and runoff, all with ramifications for stream flow (IPCC 2013; Wohl and others 2012). Although recent (2000–2010) precipitation has reversed the general drying trend in the tropics (from 1970 to 2000), the last 50 years has seen a weakening of the global monsoon circulations and a decrease in the number of days with precipitation (Zhou and others 2008), which together reduce stream flows (Piao and others 2010). The strengthening of Hadley-cell subsidence in the subtropics reduces cloud cover with resultant changes in solar radiation driving increases in potential evapotranspiration (PET). The strong relationship between tropical rainfall intensification and warming sea surface temperatures (SST) is likely to result in larger rainfall events and a reduction in light to moderate rainfall events (Lau and Wu 2011). Large inter-annual variability in Hadley and Walker circulation patterns related to El Niño Southern Oscillation (ENSO) have potentially concealed a strengthening of tropical circulation patterns since the mid-1970s (Brönniman 2009; Mitas and Clement 2005). Shifts in ocean currents and temperatures during ENSO periods result in prolonged periods of drought in tropical regions, but projections and forecasted changes in ENSO due to warming are highly uncertain due to natural variability (Kim and others 2014; Risbey and others 2014). Thus, Hawai'i experiences high inter-annual variation in precipitation, in addition to large-scale, warming-related changes in precipitation. Drought periods reduce stream flows and aquifer recharge rates, which affect freshwater availability to community and ecosystems (Meehl 1996). Reductions in freshwater supply limit stream habitats and lead to reductions in species abundance and diversity (Gingerich and Wolff 2005).

Highly variable oceanic currents and total column water vapor (TCWV) produce heterogeneous climatic conditions across the tropics and result in large seasonal and inter-annual variability in rainfall, including Hawai'i (Chu and Chen 2005; Mimura and others 2007; Strauch and others 2015). The intensity of individual rainfall events appears to be increasing as warmer air holds more moisture (Westra and others 2013), leading to greater flow variability (Milleham and others 2009; Milly and others 2002). Further, increases in the number of dry days are likely leading to a general drying of the tropics (Quan and others 2004) and an increase in solar radiation leading to increases in photosynthesis and transpiration that reduce water inputs to streams (Oliveira and others 2011). Although precipitation in the tropics often follows a strong relationship with TCWV and atmospheric convergences associated with higher SST drive precipitation patterns (Trenberth and Shea 2005), in Hawai'i, this is not always the situation as total rainfall and the magnitude of individual storm events are decreasing in some areas despite increasing SST and TCWV (Bassiouni and Oki 2012; Chen and Chu 2014). Projected increases in air and ocean temperatures for the eastern Pacific Region (Ruosteenoja and others 2003) coupled with decreased rainfall (Mimura and others 2007; Timm and Diaz 2009) are expected to affect seasonal rainfall patterns. Timm and others (2013) project that increases in SST for tropical oceans are not likely to result in a greater frequency of

extreme precipitation events in Hawai'i, although there is likely a continued downward trend in total rainfall for many regions coupled with an increased frequency of drought (Chu and others 2010). New downscaling results for Hawai'i suggest declines in average rainfall ranging from 5 to 40% depending on the season, climate scenario, and island, with a growing contrast between windward and leeward regions (Timm and others 2015).

Between 1975 and 2006, Hawai'i experienced a 0.163°C decade^{-1} increase in surface temperatures (Giambelluca and others 2008) although annual precipitation declined at a rate of 6.6% decade^{-1} over the 30 years ending in 2007 (Frazier and Giambelluca, unpublished data). An increase in drought probability, especially since the 1950s (Chu and others 2010), related to an upward trend in trade wind inversion frequency (Cao and others 2007), has been accompanied by a decrease in median baseflow in Hawaiian rivers from 1943 to 2008 compared to pre-1943 records (Bassiouni and Oki 2012).

There are numerous interactions that also require attention. For example, a diminishing vertical lapse rate could result in a more stable atmosphere, steadily drier conditions, and, because of warming driven increases in PET, reduced groundwater recharge and stream discharge (Cao and others 2007; Johnson 2012; Timm and Diaz 2009). Decreasing rainfall is also associated with reduced cloud cover, and the increase in insolation will further increase PET and reduce stream flow (Milleham and others 2009). These interactions can exert over-riding influence on watershed hydrology. In East Africa, forecasted precipitation increased with warming but modeled PET increased at a faster rate, based on the A2 emissions scenario, which when coupled with an increase in surface runoff, resulted in declining groundwater recharge and stream base flow (Milleham and others 2009). Similarly, if relative humidity remains constant with rising air temperature and SST, vapor pressure deficit will most likely increase only marginally (Foster 2001), with little effect on PET. Initial modeling in Costa Rica suggests that climate change will result in a rising cloud base during the dry season in montane tropical forests (Still and others 1999). A changing climate may also affect the contribution of cloud water interception (fog drip) to watersheds as relative humidity and the elevation of the temperature inversion layer shift.

The hydrological effects of species introduction are underappreciated, especially in the tropics (Asner and others 2008; Cavaleri and others 2014; Giambelluca and others 2009b). Plant invasion can result in monotypic stands of high water-use plants that effect the structure and function of watersheds by altering rainfall energy (Nanko and others 2013), rainfall and cloud water interception and throughfall (Giambelluca and others 2007; Mair and Fares 2010; Safeeq and Fares 2012), evapotranspiration (Giambelluca and others 2007), infiltration rates, and surface water runoff (Zhang and others 2011). Further, hydrologic responses of combined changes in CO_2, temperature, and plant physiology, are not well understood (Coe and others 2009; Knorr and others 2005) along with their potential to affect plant water use or forest structure (Cavaleri and others 2014). In Hawai'i and other tropical locations, *Psidium cattleianum* is one such rapid invader with demonstrated potential to alter watershed hydrology (Strauch and others 2016; Takahashi and others 2011). Growth of *P. cattleianum* is dependent on environmental conditions: in full sunlight, it grows more slowly as an evergreen shrub (2–4 m tall), often branching from the base with an overall round shape; under shaded conditions, *P. cattleianum* grows tall, with few branches, reaching 8 m or more. Further, the spread of *P. cattleianum* alters community composition by shading understory species and displacing epiphytic communities that influence cloud water interception (Huenneke and Vitousek 1990). In Hawai'i cloud water interception, canopy water storage, and canopy evaporation are greater in native-dominated *Metrosideros polymorpha* forest (Takahashi and others 2011), whereas throughfall decreases but stem flow increases in *P. cattleianum* invaded forest (Mair and Fares 2010; Mudd and Giambelluca 2006; Safeeq and Fares 2012; Takahashi and others 2011). An increase in stem flow may increase runoff versus infiltration in *P. cattleianum* forests, but the reduction in effective rainfall may lead to an overall reduction in groundwater recharge (Takahashi and others 2011). However, watershed scale effects are poorly quantified, and interactions with warming and drying are unknown.

To address these knowledge gaps, we examined stream flow for 88 watersheds along a highly constrained mean annual rainfall (MAR) gradient using the distributed soil hydrology vegetation model (DHSVM) for water years 2005–2012 (Wigmosta and others 1994). These adjacent watersheds represent a model hydrological study system (Strauch and others 2015), spanning a MAR range of 3000–7500 mm (Figure 1), across which mean annual temperature (same elevation range on Mauna Kea volcano), plant diversity (>85% of stand basal area dominated by one canopy species, *Metrosideros polymorpha* and one mid-story species, *Cheirodendron trigynum*), land use (closed-canopy

forest above 600 m, long-term agriculture below 600 m), soil type (all Andisols with most being Hydraudands), and parent material origin vary minimally. We used DHSVM, parameterized with Hawai'i specific vegetation and soil values, and calibrated it against locally measured stream flow, to quantify how flow responds to observed reductions in MAR across a rainfall gradient (see Appendix A). We then used DHSVM to examine how stream flow is affected by altered rainfall (current, ±20% MAR), temperature (current, +2°C), and vegetation (current plant cover, a +600 m expansion of *P. cattleianum*, watersheds fully invaded by *P. cattleianum*, and a restoration scenario with full removal of *P. cattleianum* and replacement with native forest). These climate and vegetation changes were organized into 24 scenarios representing a full factorial design (Table 1). This modeling exercise across a highly constrained 4500 mm precipitation gradient, allows us to explore hydrological responses of a tropical watershed to global change. Further, it allowed us to explore if patterns observed with drying across the MAR gradient (Strauch and others 2015) are also captured with modeled changes in MAR.

In previous work (Strauch and others 2015), reductions in rainfall across the MAR gradient caused declines in stream flow (mean annual flow, MAF; median flow, Q_{50}) and flow stability (Q_{90}:Q_{50}) but increased flow variability (Q_{10}:Q_{90}). Here we hypothesize that (1) modeled increases in temperature and decreases in rainfall would result in proportionally greater reductions in flow for lower MAR watersheds compared with higher MAR watersheds, and (2) the expansion of *P. cattleianum* would increase the absolute yield (Q_{10}Y) and relative magnitude (M_H) of high flows, while decreasing absolute yield (Q_{90}Y) and relative magnitude (M_L) of low flows. To test these hypotheses, and to understand the relative importance of these change scenarios with respect to flow, we compared model results from the 24 scenarios to results using existing vegetation and climate data. Storm flow (Q_{10}) values were calculated because maximum flows determined the design of human infrastructure (for example, bridges, culverts, diversions, and dams), but which are difficult to predict in tropical environments and expected to change. Low flows (Q_{90}) were calculated because even in humid tropical environments, seasonal and annual variation in rainfall affects water flow, which can limit agriculture, energy production, and habitat for freshwater species.

Methods

Study Area

The North Hilo and Hāmākua districts encompass the windward side of Hawai'i Island (Figure 1) and

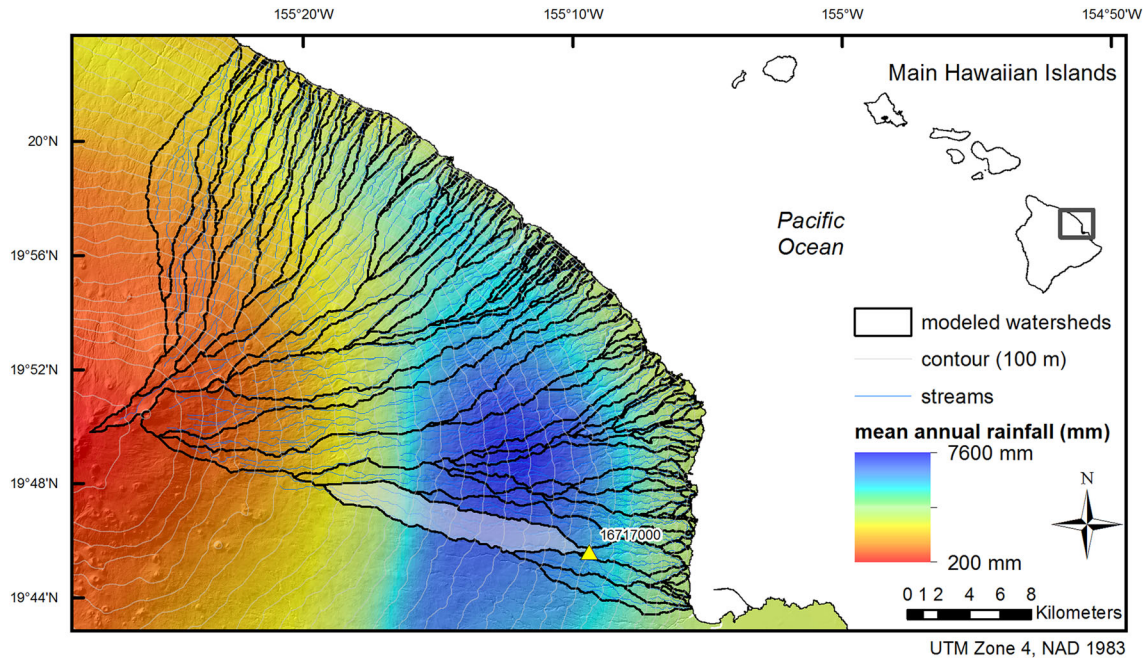

Figure 1. Map of the windward coast of Hawai'i Island with mean annual rainfall based on Giambelluca and others (2013) with the outline of 88 watersheds used. Honolii gaging station 16717000 (*triangle*) and upstream catchment (*shaded*) are provided.

Table 1. Factors for Current (Baseline) and Model Scenarios for the Windward Coast, Hawai'i Island

Factor	Baseline	Model scenarios
Temperature	Current	2°C increase
Rainfall	Current	20% less rainfall
		20% more rainfall
Vegetation scenarios	Current vegetation cover	600 m expansion of *P. cattleianum*
		Complete invasion of *P. cattleianum* below 1830 m
		Full removal of *P. cattleianum* and replacement with native vegetation

span a precipitation gradient from Hilo (6500 mm MAR) to Pa'auilo (3000 mm MAR) with a peak in Honomū (7500 mm MAR). Watersheds are characterized by narrow gulches, young soils (<100,000 years old), and native 'ōhi'a (*Metrosideros polymorpha*) dominated forests at upper elevations (>600 m a.s.l.). Lower elevations are characterized by abandoned sugar cane fields converted to homesteads, pastures, eucalyptus stands, or row crops. Vegetation at lower elevations is dominated by non-native species, including African tulip (*Spathodea campanulata*), albizia (*Falcataria moluccana*), and strawberry guava (*P. cattleianum*).

Distributed Hydrology Soils Vegetation Model Development

Watershed boundaries, stream networks, and grid cells were generated from US Geological Survey (USGS) 10-m resolution digital elevation models (DEM), which were filled to eliminate hydrologic ''sinks,'' locations where the model would not ''drain'' in a downstream direction, and conditioned to reflect actual National Hydrography Dataset (NHD) stream channel locations. Stream layers were created by varying the number of upstream pixels necessary to develop channel initiation until created stream vectors reasonably approximated networks in the NHD (Roth and Dewald 1999). Equations provided by Parker and others (2007) were used for each stream reach to estimate active channel width, active channel depth, channel gradient, and channel roughness.

Thirty-nine different vegetation and land cover types were identified from a 30-m resolution Hawai'i land cover GAP analysis (USGS 2005). To refine the GAP data to more accurately reflect the current distribution of *P. cattleianum* forest species, the relative abundance of *P. cattleianum* was modeled from an existing plot network of 50 circular subplots (30 m radius) in the Hawai'i Experimental Tropical Forest located between 540 and 1640 m in elevation (F. Hughes, unpublished data) and in the center of our study system. *Psidium cattleianum* invasion in subplots ranged from 0–58% of total basal area with approximately half (22 subplots) having *P. cattleianum*. We organized these plots into four classes of forest invasion: fully invaded (>10% basal area of *P. cattleianum*), moderate invasion (5–10% *P. cattleianum*), light invasion (0.1–5% *P. cattleianum*), and no invasion (0%). Given the relatively small diameter size of *P. cattleianum* and the cutoff value for the sampling (5 cm DBH), 10% basal area represents a sizable *P. cattleianum* invasion. As *P. cattleianum* occurrence

varies with mean annual precipitation and elevation (Jacobi and Warshauer 1992), *P. cattleianum* was modeled in the subplots with MAR (250 m resolution; Giambelluca and others 2013) and elevation (30 m resolution DEM) with the resulting significant multiple linear regression ($F = 28.3$, $P < 0.005$, $R^2 = 0.74$, $n = 20$) generally showing good agreement. Ranges in elevation and MAR used for this model were similar to that described in the study area as a whole. The model then provided an approximation for categorizing landscape-level *P. cattleianum* distribution in areas identified as forest cover in the GAP land cover dataset.

Vegetation types were linked to model parameter files that describe stand-level physical characteristics required to run the model. These characteristics control the calculation of evapotranspiration (ET), including transpiration and evaporation from the soil and wet canopy as well as incidence of sunlight on the soil surface. Parameters for canopy dynamics (max and min stomatal resistance) were estimated for both *M. polymorpha* and *P. cattleianum* based on Giambelluca and others (2007, 2009a) and Kagawa and others (2009) and scaled linearly with increasing *P. cattleianum* abundance and relative openness of stand type (see Appendix A, vegetation classes 31–39). Starting maximum and minimum stomatal resistance was 100 and 20 mmol m^{-2} s^{-1} for *M. polymorpha*, respectively, and 150 and 33 mmol m^{-2} s^{-1} for *P. cattleianum*, respectively. Soil moisture threshold, the value above which soil moisture does not restrict transpiration, and the fraction of total solar radiation as photosynthetically active shortwave radiation were assumed constant at 0.358 and 0.686, respectively. Additional parameters including stand-level percent canopy closure, root depths, leaf area index (LAI) from MODIS, and other physical factors were approximated using available literature sources and scaled linearly on the basis of vegetation type. (Asner and others 2003; Kagawa and others 2009; Waichler and others 2005). Modeled subcatchment streamflow was relatively insensitive to variation in LAI (see Appendix B).

The DHSVM also requires spatially distributed information on geology, soil texture characteristics, and soil depth which determine the rate and volume at which water moves through the soil profile in both saturated and unsaturated conditions. Soil depth and textural classes were mapped from the Natural Resources Conservation Service (NRCS) dataset (USDA 2008). One-hundred and fifty NRCS classes were combined into 16 soil types based primarily on textural class. Values needed to define each soil textural type were estimated based on published literature (Abu-Hamdeh and Reeder 2000; Coen and Wang 1989; Hantush and Kalin 2003; Saxton and Rawls 2006; USDA 2008; VanShaar and others 2002). Based on soil survey database values, we made the simplifying assumption of a uniform soil depth of 1.5 m for the project area. Base layer conductivity, groundwater conductivity, and groundwater effective porosity values specific to the 16 geologic layers were used to map groundwater contributions to stream flow (Appendix A). Water could pass below the lowest soil layer into a shallow groundwater zone, where it may be transferred back to the soil layer based on hydraulic head and vertical hydraulic conductivity values from the literature. Water could also accumulate in a deep groundwater zone where it did not return and was assumed to leave the watershed as submarine groundwater discharge to maintain mass balance.

The DHSVM is driven by meteorological data run at a subdaily (every three hour) time-step. Interpolated meteorological data included precipitation, air temperature, wind speed, relative humidity, and shortwave and longwave radiation, each of which was collected from six climate stations across the study area. Climate stations were part of the USDA Forest Service Remote Automated Weather Station (RAWS) network, the NRCS Soil Climate Analysis Network (SCAN), the NOAA weather station network, and the University of Hawai'i—USDA Forest Service Institute of Pacific Islands Forestry Vegetation Climate Observatory. Each pixel value was based on inverse distance weighted from weather stations. Periods of missing data were filled using regression analysis based on data from nearby stations. Longwave radiation was not measured at any of the stations, but was estimated from shortwave radiation, precipitation, and air temperature following the approach described by Bowling and Lettenmaier (1997). Precipitation and adjacent cell inflow inputs to each grid cell were processed at a 3-h time-step and then passed as an input to downgradient cells for the next round of calculations. Mean annual rainfall (m) was calculated as the MAR for all pixels within delineated watershed areas during the period of record (POR; water years 2005–2012). Period of record MAR values were highly correlated to watershed MAR ($R^2 = 0.93$; Figure 2A) as provided by Giambelluca and others (2013).

Fog drip (cloud water interception) can represent a significant proportion of total water input into humid tropical systems (Juvik and Ekern 1978). We did not consider fog drip for two reasons. First, the DHSVM does not account for fog drip and so

there is no parameter associated with this input. Second, there are no measurements of fog drip in our project area. Despite this, the fully parameterized model performed well during the preliminary development phase (at USGS gage 16717820 for water years 1969–1971) and during calibration runs (see below). Although we could estimate the fog drip contribution to the water budget across the MAR gradient, for example, adding 20% to the total in the intermediate areas, the error of not explicitly modeling fog drip is unlikely to create bias across modeled treatments because: (1) as MAR declines, fog drip is likely to become proportionally less important, and so modeled changes in stream flow across MAR would be conservative; (2) in wet areas, fog drip is overwhelmed by MAR; (3) the proportional contributions of fog drip are unlikely to vary strongly across modeled changes in MAR (±20% treatments); and (4) warming could affect fog drip, but data are completely lacking on these potential changes. Overall, fog drip is a poorly quantified input, varies over time and space [see Juvik and Ekern (1978) or Scholl and others (2002)], and responses to environmental change represent an important area of current climate change research.

Model Calibration and Accuracy

The DHSVM was calibrated for use in this study by optimizing model stream discharge with respect to observed values from Honoli'i stream gage (USGS stream gage number 16717000) for water years 2005–2012. The Honoli'i watershed represents a middle ground among watershed MAR. Calibration consisted of varying the lateral and vertical hydraulic conductivity values to arrive at the best fit with the observed data until the gage values were in agreement. Under current climate and vegetation patterns, we found robust agreement between modeled and observed flow (Figure 2B). Modeled mean annual flow (R^2 = 0.99) and mean monthly flow (R^2 = 0.92) correlated well with observed values while at a daily resolution, the model performed well (R^2 = 0.62) but tended to underestimate peak flows during large storm events and overestimate flow in the recession limb of the hydrograph.

Model Scenarios

Following calibration, DHSVM was run under a full factorial of 24 different scenarios (Table 1). Scenarios were developed based on predicted changes in temperature, the range of possible changes to rainfall, and anticipated changes in vegetation cover based on assumptions of no management or greatly expanded management. Each climate-related scenario included either the current temperature pattern or a constant 2°C increase in temperature applied to the temperature record. A 2°C, temperature increase represents a reasonable approximation of late 21st century climate in the North Pacific under a business as usual emissions pathway (IPCC 2013). Relative humidity was held constant with this temperature increase. The effect of uncertain future precipitation change was assessed using scenarios of 20% increase, no change, and 20% decrease. We did not have access to dynamically downscaled temperature and rainfall data that would allow us to explore future changes in the temporal distribution of MAR. Vegetation scenarios included the current modeled distribution of *P. cattleianum*, a +600 m expansion of *P. cattleianum* into native forest from the boundary of its current distribution, complete invasion by *P. cattleianum* of native forests below 1828 m elevation, and a restoration scenario with removal of *P. cattleianum* from currently invaded forests and replacement with native only plant species forest. Vegetation was reclassified using the original class of *P. cattleianum* invasion and slope distances from pixels with any *P. cattleianum* invasion, reflecting an increase in *P. cattleianum* biomass, stem density, and changes in canopy closure (see Appendix C). Some forest areas are already experiencing complete invasion, while a +600 m expansion represents a conservative estimate of invasion expansion by 2050. Watershed managers are working on various physical, chemical, and biocontrol techniques to greatly reduce the growth and spread of *P. cattleianum* across its current range.

Data Analysis

Flow metrics and mean annual flow were calculated for each stream based on flow data generated with a 3-h time-step and converted to mm to normalize by watershed area. We computed storm flow, the magnitude of the flow equaled or exceeded 10% of the time (Q_{10}), the mean magnitude of the annual high flow relative to the median flow (M_H), the magnitude of the median flow (Q_{50}), mean annual flow (MAF), low flow, the magnitude of the flow equaled or exceeded 90% of the time (Q_{90}), the mean magnitude of the annual low flow relative to the median flow (M_L), flow variability, the ratio of high flow to low flow (Q_{10}:Q_{90}) and flow stability (Q_{90}:Q_{50}), the ratio of low flow to median flow, for each watershed (Clausen and Biggs 2000; Olden and Poff 2003). Relationships between watershed MAR and Q_{10} yield (Q_{10}Y), Q_{50} yield (Q_{50}Y), Q_{90} yield (Q_{90}Y), as well as between

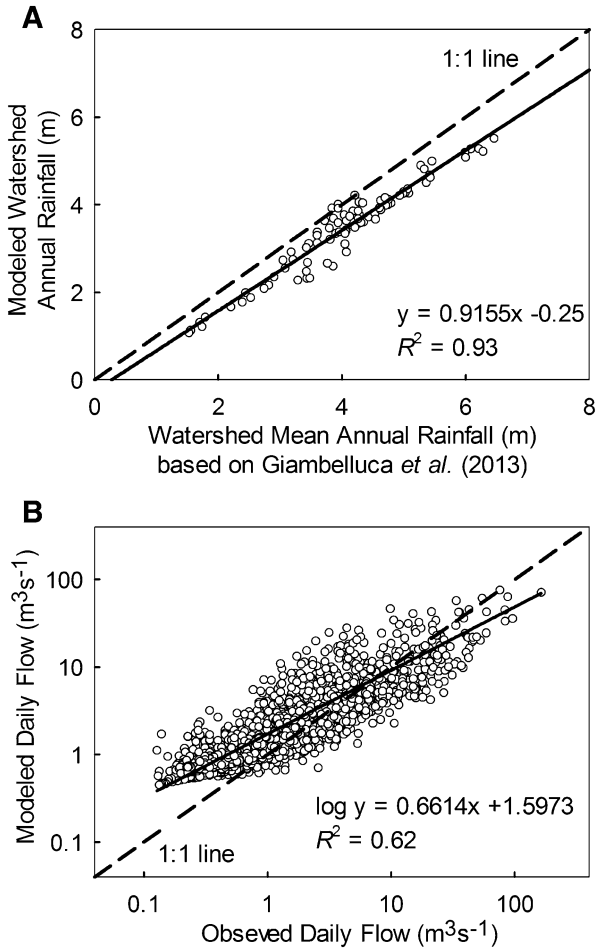

Figure 2. **A** Modeled watershed mean annual rainfall compared to long-term watershed mean annual rainfall based on Giambelluca and others (2013) for water years 2005–2012. **B** Observed and modeled mean daily flow from water years 2005–2012 at the USGS gage station number 16717000 on Honoli'i River, Hawai'i Island.

M_H, M_L, and Q_{10}:Q_{90} to log-transformed volumetric MAR were examined using least-squares linear regression with SimgaPlot (v. 12.0, Systat Inc., San Jose, CA). All flow values were log-transformed to maintain normally distributed residuals. Similarly, we used linear regression forced through zero to examine the effect of modeled changes in climate, invasion or restoration, and rainfall on MAF (as mm y^{-1}) and reported the slope (β) with the current period of record MAR for each model. The ratio of scenario modeled regression coefficient (β) to modeled current conditions regression coefficient ($\beta_{current}$) was calculated for comparison. The median percent (%) change in MAF and the total cumulative change in MAF across all watersheds were also calculated. To visualize spatial differences in stream flow across the study region, we utilized a geographic information system (GIS) to depict flow metrics under current conditions and the percent change in MAF from current conditions for each scenario.

Results

Modeled Flow Across a Natural Climate Gradient

With increasing annual rainfall, we found an increase in Q_{90} (R^2 = 0.68 $F_{1,86}$ = 181.7, $P < 0.001$), Q_{50} (R^2 = 0.77 $F_{1,86}$ = 293.8, $P < 0.001$), Q_{10} (R^2 = 0.71, $F_{1,86}$ = 211.7, $P < 0.001$), and MAF (R^2 = 0.73 $F_{1,86}$ = 234.3, $P < 0.001$) (Figure 3A–C). Flow stability was negatively correlated with MAR (R^2 = 0.30, $F_{1,86}$ = 36.9, $P < 0.001$); as watersheds became drier, flow become more unstable (Figure 3D). This occurred due to reductions in low flow with declining MAR, whereas the intensity of major rainfall events did not change with MAR. There was little change in M_H and M_L across the MAR gradient (Figure 3F), even though absolute flow yields did not follow this trend (Figure 3A–C). Across the model hydrological study system, trends in flow statistics generally followed precipitation patterns (Figure 4A–C), as expected, but intermediate MAR watersheds presented the most variable flows (Figure 4D).

Modeled Flow and Climate Warming Under Current Vegetation

A modeled 2°C increase in temperature (+2°C treatment) alone had the smallest effect on flow, with a mean % change in Q_{50}Y and mean MAF of +1.89% (SE ± 0.13%) and +1.66% (SE ± 0.09%), respectively. This resulted in a mean change in MAF of 0.005 m^3s^{-1} (SE ± 0.0008 m^3s^{-1}) and a cumulative gain of 14.61 million m^3s^{-1} (Table 2). The amount of water gained in MAF in this scenario increased with increasing MAR (R^2 = 0.99, $F_{1,86}$ = 6199, $P < 0.001$) although low MAR watersheds had the largest percentage gains in MAF (Figure 5A). Compared to current conditions, the +2°C increase resulted in a slight reduction in M_H and a slight increase M_L.

Increased stream flow in response to warming may be due to reductions in stomatal conductance, a response in plants that helps reduce moisture loss and that would lead to an increase in soil water. Further, the modest increase in the vapor pressure deficit (VPD) resulted in higher evaporative demand with the stomatal conductance response to increasing VPD strong enough to

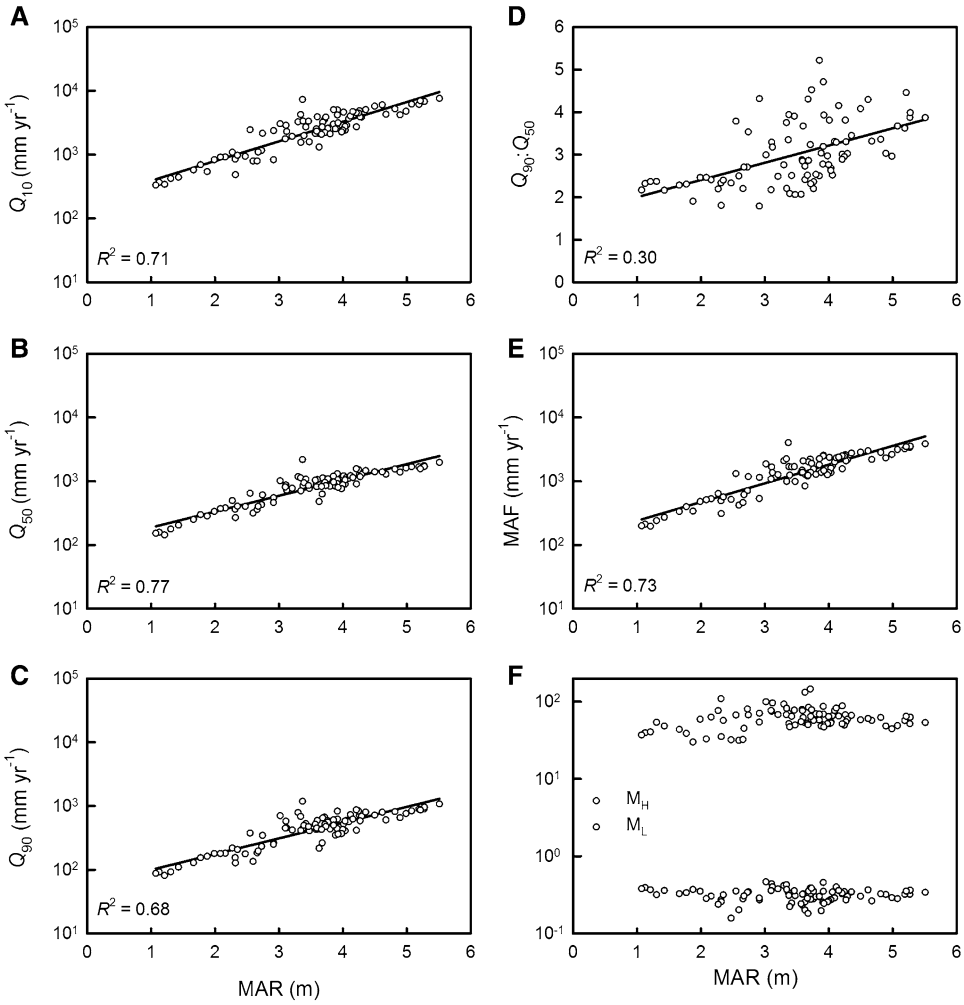

Figure 3. Under current conditions, (**A**) high flow (Q_{10}), (**B**), median flow (Q_{50}), and (**C**), low flow (Q_{90}) versus period of record mean annual rainfall (MAR). Also, (**D**) flow stability (Q_{90}:Q_{50}) (**E**) mean annual flow (MAF) and (**F**) relative magnitude (unitless) of the mean annual low flow (M_L) or high flow (M_H) versus MAR.

overcome the increase in PET, reducing transpiration and ET overall. Although *P. cattleianum* transpiration increased in this scenario, current *P. cattleianum* cover is relatively small compared to *M. polymorpha* in most watersheds. This indirect effect on plant water use by temperature (via VPD) would be more subject to real world changes to insolation, relative humidity and downwelling longwave radiation, which because of lack of data, were kept constant across modeling scenarios. Additional consequences of temperature increase, (for example, effects on TCWV or on the height of the inversion layer) also were not included in this analysis.

Modeled Flow and Altered Rainfall Under Current Vegetation

Both decreased and increased precipitation scenarios had unsurprisingly large effects on flow (Strauch and others 2015), with greater absolute changes to MAF occurring in wetter, high flow watersheds, while drier, low flow watersheds had the greatest % change in flow (Figure 6A). A 20% decrease in rainfall resulted in a mean change in MAF of −33.6% (SE ± 0.53%) over the 8-year period, with a range of −26.3 to −49.8%. By comparison, a 20% increase in rainfall resulted in a mean change in MAF of 38.1% (SE ± 0.94%) with a range of 26.9–69.5% (Figure 6B). The combined effects of the +2°C and −20% rainfall resulted in a change in mean annual flow of −32.2% (SE ± 0.48%) with % change in annual flow increasing with decreasing MAR ($F_{1,86}$ = 56.8, $P < 0.0001$; Figure 7A). The largest regression slopes between MAF yield and MAR were in the +20% rainfall scenarios while the smallest slopes were in the −20% rainfall scenarios (Table 2).

Modeled Flow and Effects of *P. cattleianum* Invasion

Modeled +600 m expansion in *P. cattleianum* and complete invasion of watersheds below 1830 m

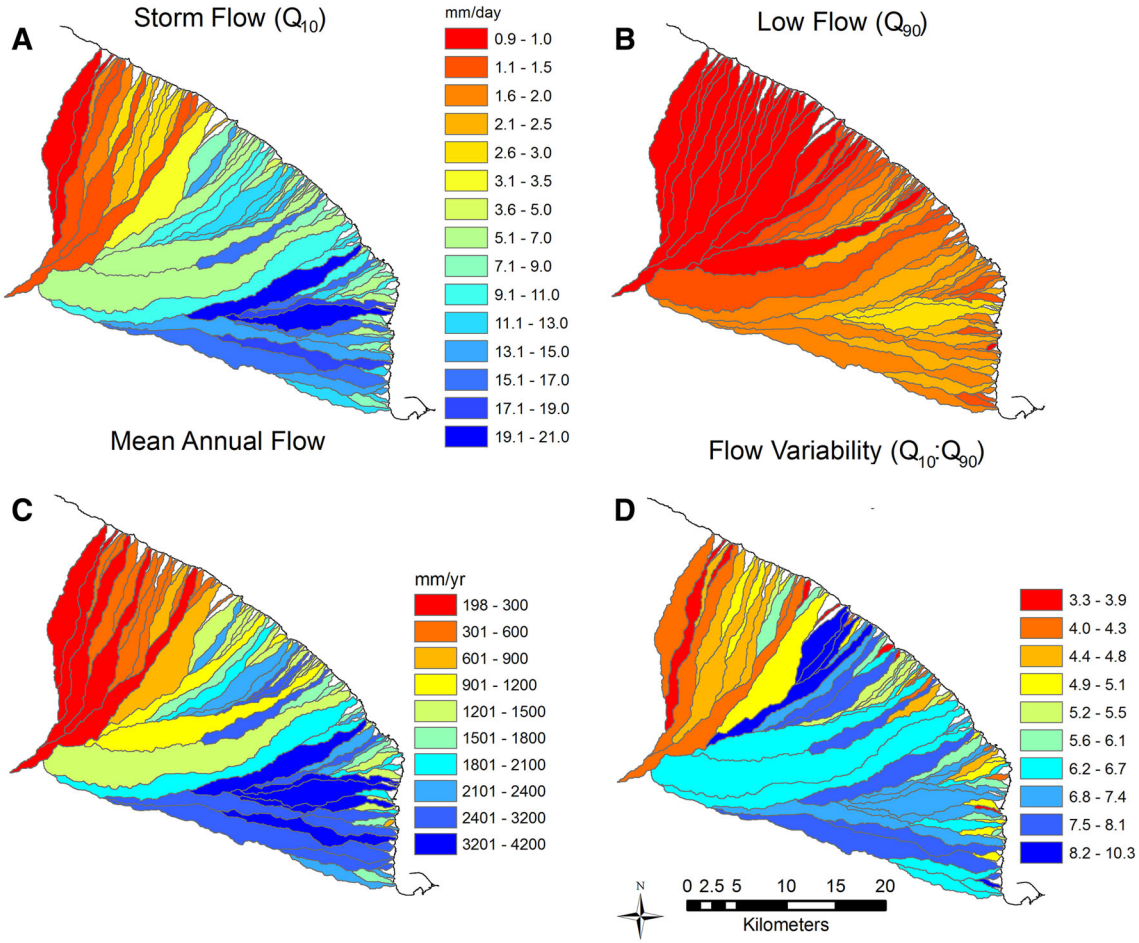

Figure 4. Current conditions modeled (**A**) storm flow (Q_{10}; mm d^{-1}), (**B**) low flow (Q_{90}; mm d^{-1}), (**C**) mean annual flow (mm y^{-1}), and (**D**) flow variability (Q_{10}:Q_{90}) for watersheds on the windward coast of Hawai'i Island for water years 2005–2012. Top *color gradient* applicable for (**A**) and (**B**).

a.s.l. resulted in −0.92% (SE ± 0.07%) and −1.85% (SE ± 0.03%) mean changes in MAF, respectively, equating to 10.69 and 21.45 million m^3 of less streamflow per year (Table 2; Figure 5B, C). With complete invasion of forests, mean change in Q_{90} was −2.53% (SE ± 0.46%) ranging from −14.0 to 5.3%, whereas mean change in Q_{10} was −1.64% (SE ± 0.29) ranging from −11.2 to 2.16%. Further, there was a mean % change in M_H of +1.73% (SE ± 0.42%) ranging from −20.5 to 12.4%, and a mean % change in M_L of −0.64% (SE ± 0.65) ranging from −12.2 to 24.8%. Full restoration of native vegetation increased mean MAF by 1.03% (SE ± 0.09%) resulting in a return of 14.99 million m^3 y^{-1} (Figure 5D), whereas increasing M_L by a mean of 1.13% (SE ± 0.69%; range −18.8 to 34.9%) and decreasing M_H by a mean of 0.83% (SE ± 0.31%; range −4.3 to 22.9%).

With increasing *P. cattleianum* vegetation cover, the rate of change in mean annual flow yield decreased with MAR, suggesting a negative effect of *P. cattleianum* on the watershed response to rainfall. Physiological differences between native and introduced species are likely to influence the movement of water through watersheds. In Hawai'i, *M. polymorpha*-dominated forests are being replaced by *P. cattleianum*-dominated forests, resulting in a 27% greater ET during wet conditions and a 53% greater ET during dry conditions (Giambelluca and others 2007). Throughfall rates in *P. cattleianum*-dominated forests in drier environments are much lower than native forests due to increases in wet-canopy evaporation and stemflow (Mair and Fares 2010).

Combined Effects of *P. cattleianum* Invasion, Warming, and Rainfall Change

Compared to current climate and forest cover conditions, a +2°C and complete *P. cattleianum*

Table 2. Regression Coefficient (β) of Each Linear Regression Model Between Mean Annual Flow (MAF) (mm y^{-1}) and Period of Record Mean Annual Rainfall (mm) with the Ratio of Modeled Scenario Regression Coefficient (β) to Current Conditions Regression Coefficient ($\beta_{current}$).

Scenario			Mean annual flow yield		Median (SD) Δ MAF	Total Δ MAF
Temp	Rainfall	Vegetation	β	β / $\beta_{current}$	(m^3 s^{-1})	(m^3 s^{-1})
Current	+20%	Full restoration	0.6546	1.3409	0.0509 (0.2375)	13.129
Current	+20%	Current	0.6498	1.3310	0.0498 (0.2274)	12.644
Current	+20%	+600 m	0.6467	1.3246	0.0485 (0.2213)	12.279
Current	+20%	Full invasion	0.6457	1.3227	0.0479 (0.2178)	11.908
Current	Current	Full restoration	0.4929	1.0097	0.0013 (0.0102)	0.475
Current	Current	Current	0.4882	1.0000	n/a	n/a
Current	Current	+600 m	0.4855	0.9946	−0.0013 (0.0062)	−0.3388
Current	Current	Full invasion	0.4845	0.9924	−0.0004 (0.0156)	−0.6797
Current	−20%	Full restoration	0.3424	0.7014	−0.0434 (0.2091)	−11.392
Current	−20%	Current	0.3380	0.6924	−0.0453 (0.2190)	−11.855
Current	−20%	+600 m	0.3356	0.6874	−0.0463 (0.2246)	−12.167
Current	−20%	Full invasion	0.3348	0.6857	−0.0480 (0.2275)	−12.445
+2°C	+20%	Full restoration	0.6591	1.3502	0.0542 (0.2437)	13.479
+2°C	+20%	Current	0.6560	1.3438	0.0532 (0.2353)	13.144
+2°C	+20%	+600 m	0.6527	1.3369	0.0514 (0.2294)	12.798
+2°C	+20%	Full invasion	0.6528	1.3371	0.0498 (0.2271)	12.561
+2°C	Current	Full restoration	0.4971	1.0183	0.0031 (0.0148)	0.7956
+2°C	Current	Current	0.4940	1.0120	0.0019 (0.0077)	0.4630
+2°C	Current	+600 m	0.4882	1.0000	0.0007 (0.0028)	0.1455
+2°C	Current	Full invasion	0.4914	1.0066	0.0008 (0.0085)	−0.0698
+2°C	−20%	Full restoration	0.3461	0.7090	−0.0422 (0.2049)	−11.112
+2°C	−20%	Current	0.3432	0.7030	−0.0438 (0.2119)	−11.432
+2°C	−20%	+600 m	0.3407	0.6978	−0.0442 (0.2173)	−11.723
+2°C	−20%	Full invasion	0.3408	0.6980	−0.0448 (0.2190)	−11.903

Median and standard deviation (SD) change (Δ) in MAF (millions m^3s^{-1}) and total change (Δ) in mean annual flow (millions m^3s^{-1}) from current conditions for each scenario

invasion resulted in a mean % change in Q_{90} of −0.015% (SE ± 0.33%) and in Q_{10} of +0.45% (SE ± 0.25%). Subsequently the mean change in MAF was −0.001 m^3s^{-1} (SE ± 0.0009) resulting in a mean total annual reduction in streamflow of 17.6 million m^3s^{-1} across watersheds (Figure 7H). Compared to observed hydrology under current climate and vegetation conditions, modeled hydrology under +2°C and full *P. cattleianum* invasion scenarios (Figure 7H) lowered median MAF by −0.9% resulting in a reduction of 0.0698 m^3s^{-1} (Table 2). Compared to the +2°C scenario alone, +2°C and complete invasion resulted in a mean % change in M_L and M_H of −0.89% (SE ± 0.59%) and +1.50% (SE ± 0.27), respectively, as well as an increase in MAF with increasing MAR (R^2 = 0.43; $F_{1,86}$ = 19.35, $P < 0.001$). Percent reduction in stream flow under the combined effects of +2°C and invasion was greatest in lower MAR watersheds (Figure 7G, H), with differences across the gradient more pronounced under the +2°C/−20% rainfall/fully invaded scenario (Figure 7B) than the +2°C/−20% rainfall scenario alone (not shown). In the worst case scenario of +2°C/−20% rainfall/full invasion, there was a mean % change in Q_{10} of −27.5% (SE ± 0.9%) and Q_{90} of −34.8% (SE ± 0.5%). Under current rainfall with a +2°C warming, mean change in MAF for the full removal scenario was 0.01 m^3s^{-1} (2.1%), compared to the full invasion scenario which was −0.001 m^3s^{-1} (−0.3%) (Figure 7H, I).

Discussion

Managing for the continued capacity of tropical landscapes to provide clean, fresh water to society and for terrestrial, aquatic, and near-shore habitat needs has become a major natural resource challenge in island systems because watersheds and aquifers are typically smaller, and hydraulic pro-

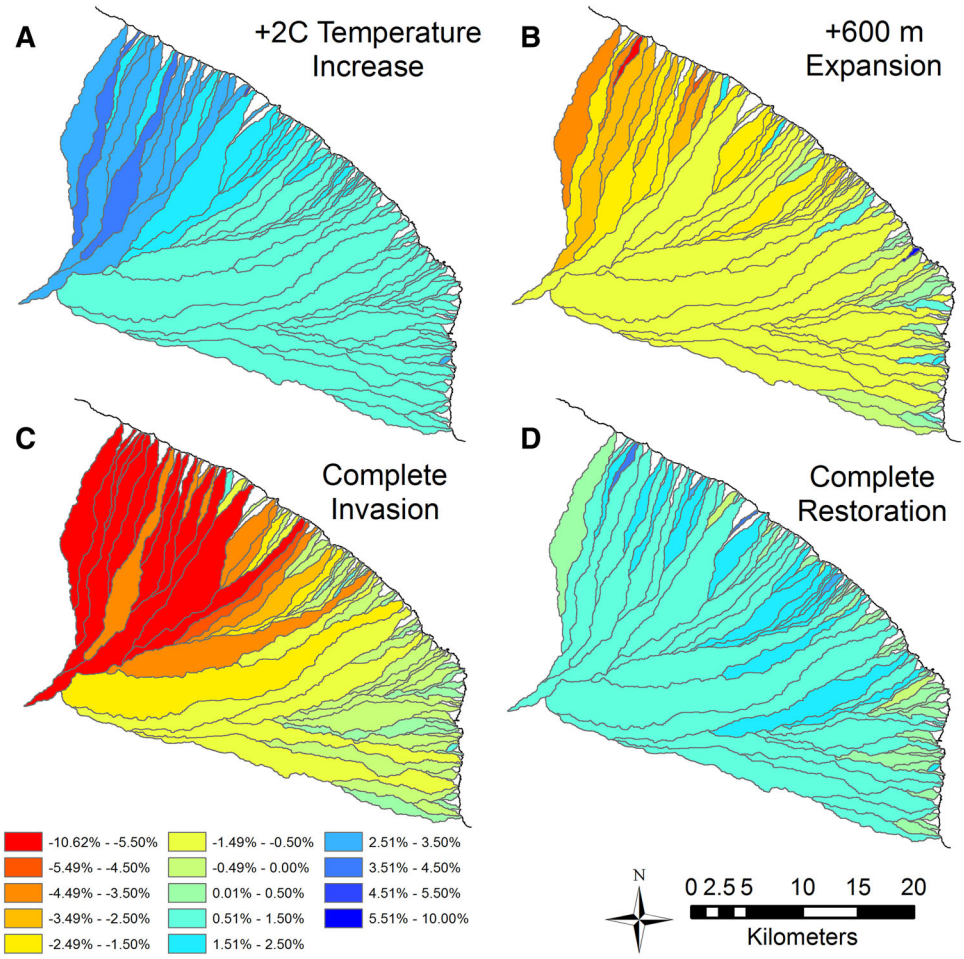

Figure 5. Modeled percent (%) change in mean annual flow for (**A**) +2°C temperature increase with current vegetation cover and current temperatures with (**B**) +600 m expansion of *P. cattleianum*, (**C**) complete invasion of *P. cattleianum*, (**D**) complete restoration to native forest, for watersheds on the windward coast of Hawai'i Island for water years 2005–2012. Legend applicable to all maps.

cesses more vulnerable to climate and land cover change. Climate change is expected to alter the spatial distribution of rainfall as well as the frequency and intensity of rainfall events on tropical islands. These changes will have consequences for watershed hydrology, but the nature of how these changes interact with land cover change has received insufficient attention. We applied DHSVM across a model hydrological study system characterized by a steep rainfall gradient to examine how stream flow may respond to the independent and interactive consequences of climate change and *P. cattleianum* invasion. Declines in watershed MAR resulted in decreases in storm, median, and low flow yields, along with decreases in flow stability and increases in flow variability. Although the full effect of these changes in water flow and flow variability on ecological processes is largely unknown for tropical island systems (Wohl and others 2012), it is clear that reduced stream flow has negative consequences for native habitat availability and freshwater biota in Hawai'i (Gingerich and Wolff 2005; McIntosh and others 2008).

Stream Flow Responses to Observed Changes in Mean Annual Rainfall

Our analyses show that declines in MAR correlate with declines in flow yield under all modeled climate scenarios, and that a warmer, drier climate will have significant and substantial negative effects on stream flow. Observed changes in MAR also exerted strong effects on flow variability, M_H, and M_L due to MAR-driven shifts in low flow and median flow. We found that drier MAR watersheds tended to have greater solar radiation and ET, reducing groundwater recharge and lower flows while the size of large storm events is less influenced by MAR (Timm and others 2011). At the same time, MAR had weaker effects on absolute changes in low flow and storm flow. Modeled *P. cattleianum* expansion reduced flow yields, but this reduction was dwarfed by the reductions due to a simulated 20% decrease in MAR. The effects of changing MAR or land cover varied across the MAR gradient, but full removal of *P. cattleianum* and replacement with forests composed entirely of native plant species increased stream flow.

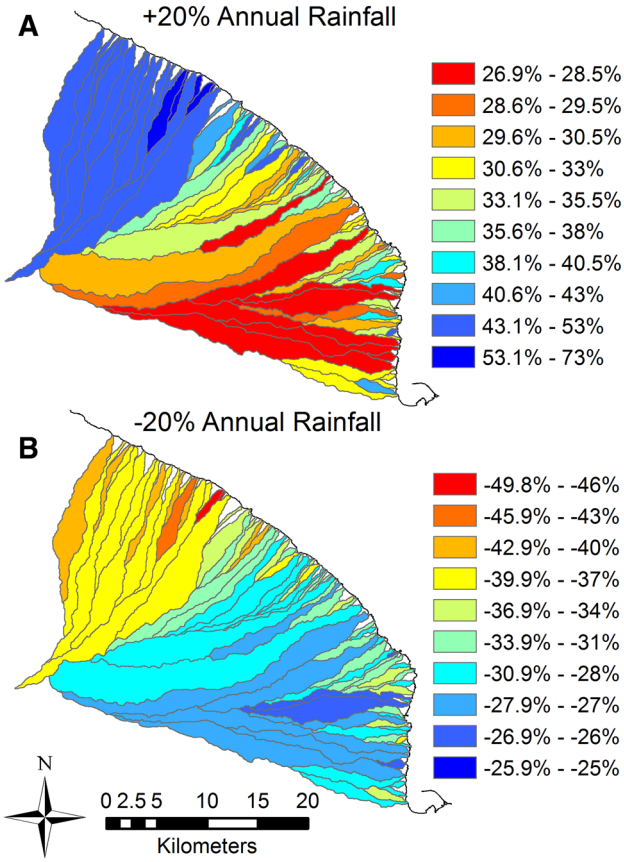

Figure 6. Modeled percent (%) change in mean annual flow for (**A**) +20% increase in annual rainfall and (**B**) 20% decrease in annual rainfall for watersheds on the windward coast of Hawai'i Island for water years 2005–2012.

Modeled Effects of Invasive Species Expansion on Stream Flow

The expansion of *P. cattleianum* into native wet forests has diverse consequences for Hawaiian ecosystems including loss of habitat for native species, new habitats for introduced species, changes in canopy structure and groundcover, and altered watershed hydrology (Strauch and others 2016). The distribution of *P. cattleianum* is primarily limited by elevation (temperature) and rainfall, with no natural herbivore or disease constraints in Hawaiian forests (Huenneke and Vitousek 1990). Little is known about the hydrologic effect of invasion by *P. cattleianum* under future climate conditions, although the maximum habitable elevation will increase with increasing temperature. In this study, modeled *P. cattleianum* expansion (+600 m from current distribution) and complete invasion of watersheds below 1830 m a.s.l. resulted in a mean MAF reduction of 0.339 and 0.680 m^3s^{-1}, respectively. With complete invasion, M_H decreased with increasing watershed MAR although at almost the same rate as for current conditions, while M_L decreased at a faster rate with increasing MAR. This suggests that the relative size of high flows may not change with invasion, although we had anticipated that increases in stem flow may increase runoff and thus high flows. Further, with increasing MAR, the rate of change in M_L was smaller with *P. cattleianum* invasion suggesting a reduction in the shallow groundwater recharge that contributes to lower flows. It is also likely that the extreme amounts of rainfall and runoff produced by many storm events may be obscuring any effects of vegetation change on hydrological properties of watersheds.

Psidium cattleianum growth rate responds more rapidly to water availability, out growing native species, and altering the structure of Hawaiian forests (Asner and others 2008). The invasion of *P. cattleianum* reduces epiphyte biomass by as much as 2.5×, reducing by approximately half the capacity of forests to capture cloud water and retain water aboveground (Mudd and Giambelluca 2006). In native forests, understory vegetation increases cloud water interception and retains fog drip and rainfall as aboveground water storage—water that contributes to stream flow and aquifer recharge (Takahashi and others 2011). The loss of understory vegetation that accompanies invasion may also drive a reduction in infiltration, leading to an increase in overland flow and sediment runoff

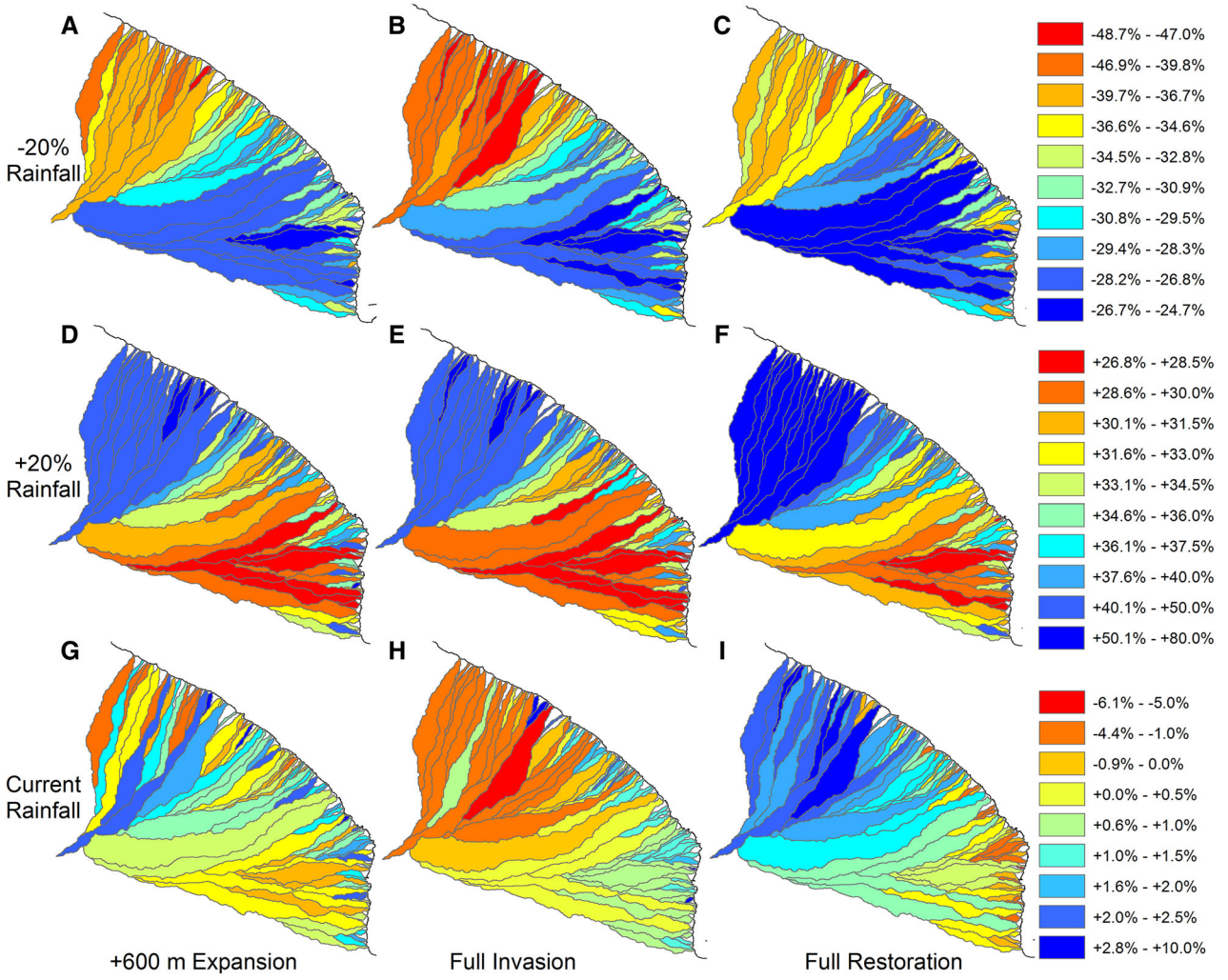

Figure 7. Modeled percent (%) change in mean annual flow for +2°C temperature increase and three potential outcomes of *P. cattleianum* management (+600 m expansion, complete invasion, and complete restoration) with three potential rainfall scenarios (−20% annual rainfall, +20% annual rainfall, and current rainfall) in watersheds on the windward coast of Hawai'i Island for water years 2005–2012. *Color gradients* are applicable to the three figures in each row.

following storm events (Zimmerman and others 2008). Further, the osmotic adjustments made by the leaves of *P. cattleianum* enable this species to endure greater negative water potentials, such that *P. cattleianum* can retain its leaves during drought periods without xylem cavitation (Yazaki and others 2010). This allows *P. cattleianum* to rapidly utilize water when it becomes available. *Psidium cattleianum* invasion increases forest growth rates and biomass accumulation, especially under shaded conditions (Ortega and others 2006; Uowolo and Denslow 2008), with subsequent shading and competition for resources by introduced species (Baruch and Goldstein 1999). In the longer-term, *P. cattleianum* serves as a food source for a variety of introduced birds and ungulates (Diong 1982; Huenneke and Vitousek 1990) as well as invertebrates (Joe and Daehler 2008) .

Combined Consequences of Climate and Species Invasion

Invasion of watersheds by *P. cattleianum* magnified the effects of climate change by further reducing low flows and increasing high flows. In the +2°C/−20% rainfall with full invasion scenario, there was a strong (R^2 = 0.87) negative relationship between Q_{10}:Q_{90} and MAR suggesting an increase in flow variability as the climate dries. By contrast, full removal treatment under the +2°C temperature scenario increased median percent change in MAF by 1.97% resulting in an increase in streamflow

across most watersheds. Modeled future climate scenarios did not consider a change in the distribution of rainfall, merely the percent change in the total amount of rainfall at each time interval. The intensity of rainfall events, the length of dry periods, or the seasonal/diel distribution of rainfall was not changed, although these are expected to change in Hawai'i and throughout the tropics (Chu and others 2010; Milly and others 2002; Quan and others 2004). Fog drip will similarly be expected to change with climate, but how and to what extent is unknown. Managing vegetation will have a small but critically important effect on increasing the supply of freshwater during periods of climate uncertainty.

Difficulties with Modeling Stream Flow in Tropical Island Systems

There are a number of inherent difficulties with modeling stream flow in tropical environments, especially where streams dissect volcanic geology and daily rainfall is extremely variable (Dettinger and Diaz 2000; Post and Jakeman 1999). Hydrographs of low-order tropical streams are very flashy, with frequent extreme flows but few intermediate flows as a result of rainfall-driven runoff events (Smith and others 1998). Understanding changes in extreme flows is important for maintaining resilient infrastructure (which is designed for flood events), quantifying erosion (most of which occurs during flood events), and for assessing effects on amphidromous species (which depend on floods for reproductive success). Here, DHSVM consistently under-predicted peak discharge of storm events, but over-predicted the recession limb of the hydrograph. This may be due to the short, narrow, and steep nature of island watersheds that move water efficiently off the landscape resulting in more steeply sloped hydrographs (time to peak flow within hours) compared to continental systems (Tomlinson and De Carlo 2003). Cuo and others (2006) similarly found that DHSVM under reported high flow events in Thailand.

The high permeability of basaltic substrates on young volcanic islands was assumed to prevent the development of freshwater lenses with heads greater than a few meters above sea level. In these model runs, we assumed some interaction with groundwater but ignored the effects of dike formation or perched water bodies. However, basalt substrates can be fully saturated at higher elevations (up to 1000 m a.s.l.) with vertical dike formations forcing the water table much closer to the land surface and making a significant contribution to stream flow (Gingerich 1999). The extent of dike formations on the windward coast of Hawai'i Island is largely unknown (Stearns and Macdonald 1946) and so this was ignored. However, water mass balance was maintained by losses to submarine groundwater discharge and the DHSVM provided good representation across a range of stream flow conditions. The model was calibrated using data from a watershed with a high MAR, so it is possible that in much drier conditions (that is, with watersheds with half the modeled MAR), the model is less accurate, although consistency in soil properties, underlying geology, and vegetation is likely to mitigate this issue.

Taken together, the value of these results may relate most to relative comparisons across scenarios and represent conservative estimates of flow and the magnitudes of extreme high and low flows. In future model runs, limiting the time-step to one hour would improve the model response to ''flashy'' environments. The use of a three-hour time-step smoothed out this type of response. Alternatively, quantifying water mass balance using a daily time-step might be more accurate, as daily values in rainfall, ET, and radiation can be generated more easily across variable topography. For future climatic scenarios, taking into account changes to the temporal distribution of rainfall may also improve the model's ability to predict changes in stream flow.

We conclude that given these future climate and vegetation scenarios: (1) the volume of water lost in high MAR watersheds under warming and drying will be substantial; (2) rivers in drier regions will lose a greater proportion of stream flow and have more variable flows than in wetter regions; and (3) increasing *P. cattleianum* cover will reduce flow volume but increase flow variability. In a warmer climate (+2°C), species invasion (fully invaded) resulted in more than a 6× reduction in mean MAF compared to current vegetation, and restoring native vegetation mitigated the effects of *P. cattleianum* on stream flow by almost doubling mean MAF. By predicting where water loss will be greatest under future climate and land cover scenarios, targeted approaches to native forest restoration will provide the most cost-effective improvements to provisioning of hydrological services.

ACKNOWLEDGEMENTS

R. Tingley and V. Keener provided useful suggestions in the development of this manuscript. This

work was made possible through USDA Forest Service Research Joint Venture Agreements with the University of Hawai'i and with the Watershed Professionals Network. Funding support for this research came from the USDA Forest Service including: Region 5 Science, Technology and Development Program, State and Private Forestry; Forest Service Research and Development Climate Change Program; and the Pacific Southwest Research Station.

REFERENCES

Abu-Hamdeh NH, Reeder RC. 2000. Soil thermal conductivity effects of density, moisture, salt concentration, and organic matter. Soil Science Society of America Journal 64(4):1285–90.

Asner GP, Hughes RF, Vitousek PM, Knapp DE, Kennedy-Bowdoin T, Boardman J, Martin RE, Eastwood M, Green RO. 2008. Invasive plants transform the three-dimensional structure of rain forests. Proceedings of the National Academy of Sciences 105(11):4519–23.

Asner GP, Scurlock JM, Hicke JA. 2003. Global synthesis of leaf area index observations: implications for ecological and remote sensing studies. Global Ecology & Biogeography 12:191–205.

Baruch Z, Goldstein G. 1999. Leaf construction cost, nutrient concentration, and net CO_2 assimilation of native and invasive species in Hawaii. Oecologia 121:183–92.

Bassiouni M, Oki DS. 2012. Trends and shifts in streamflow in Hawai'i, 1913–2008. Hydrological Processes 27(10):1484–500.

Bowling LC, Lettenmaier DP. 1997. Evaluation of the effects of forest roads on streamflow in Hard and Ware Creeks, Washington. Water resources series technical report. Seattle: University of Washington. p 189.

Brönniman S. 2009. Early twentieth-century warming. Nature Geoscience 2:735–6.

Cao G, Giambelluca TW, Stevens DE, Schroeder TA. 2007. Inversion variability in the Hawaiian trade wind regime. Journal of Climate 20:1145–60.

Cavaleri MA, Ostertag R, Cordell S, Sack L. 2014. Native trees show conservative water use relative to invasive trees: results from a removal experiment in a Hawaiian wet forest. Conservation Physiology 2:1–14.

Chapin FSIII, Carpenter SR, Kofinas GP, Folke C, Abel N, Clark WC, Olsson P, Smith DMS, Walker B, Young OR et al. 2010. Ecosystem stewardship: sustainability strategies for a rapidly changing planet. Trends in Ecology and Evolution 25(4):241–9.

Chen YR, Chu P-S. 2014. Trends in precipitation extremes and return levels in the Hawaiian Islands under a changing climate. International Journal of Climatology 34:3913–25.

Chu P-S, Chen YR, Schroeder TA. 2010. Changes in precipitation extremes in the Hawaiian Islands in a warming climate. Journal of Climate 23:4881–900.

Chu PS, Chen H. 2005. Interannual and interdecadal rainfall variations in the Hawaiian Islands. Journal of Climate 18:4796–813.

Clausen B, Biggs BJF. 2000. Flow indices for ecological studies in temperate streams: groupings based on covariance. Journal of Hydrology 237(3–4):184–97.

Coe MT, Costa MH, Soares-Filho BS. 2009. The influence of historical and potential future deforestation on the stream flow of the Amazon River-land surface processes and atmospheric feedbacks. Journal of Hydrology 369:165–74.

Coen GM, Wang C. 1989. Estimating vertical saturated hydraulic conductivity from soil morphology in Alberta. Canadian Journal of Soil Science 69(1):1–16.

Cuo L, Giambelluca TW, Ziegler AD, Nullet M. 2006. Use of the distributed hydrology soil vegetation model to study road effects on hydrological processes in Pang Khum Experimental Watershed, northern Thailand. Forest Ecology and Management 224:81–94.

Dettinger MD, Diaz HF. 2000. Global characteristics of stream flow seasonality and variability. Journal of Hydrometeorology 1:289–310.

Diong CH. 1982. Population biology and management of the feral pig (*Sus scrofa* L.) in Kipahulu Valley, Maui. Honolulu (Hawai'i): University of Hawai'i. p 431.

Foster P. 2001. The potential negative impacts of global climate change on tropical montane cloud forests. Earth Science Reviews 55:73–106.

Giambelluca TW, Asner GP, Martin RE, Nullet MA, Huang M, DeLay JK, Mudd RG, Takahashi M. 2007. Impacts of alien tree invasion on evaporation in tropical montane cloud forest in Hawaii. Eos Transactions 88:H211.

Giambelluca TW, Chen Q, Frazier AG, Price JP, Chen Y-L, Chu P-S, Eischeid JK, Delparte DM. 2013. Online rainfall Atlas of Hawai'i. Bulletin of the American Meteorological Society 94:313–16.

Giambelluca TW, Diaz HF, Luke MSA. 2008. Secular temperature changes in Hawai'i. Geophysical Research Letters 35:L12702.

Giambelluca TW, Martin RE, Asner GP, Huang M, Mudd RG, Nullet MA, DeLay JK, Foote D. 2009a. Evapotranspiration and energy balance of native wet montane cloud forest in Hawai'i. Agricultural and Forest Meteorology 149:230–43.

Giambelluca TW, Sutherland RA, Nanko K, Mudd RG, Ziegler AD. 2009b. Effects of *Miconia* on hydrology: a first approximation. International Miconia Conference. Maui, Hawaii.

Gingerich SB. 1999. Ground-water occurrence and contribution to streamflow, Northeast Maui, Hawaii. US Geological Survey. No. 99-4090.

Gingerich SB, Wolff RH. 2005. Effects of surface-water diversions on habitat availability for native macrofauna, Northeast Maui, Hawaii. Denver (CO): US Geological Survey.

Hantush MH, Kalin L. 2003. Modeling uncertainty of runoff and sediment yield using a distributed hydrologic model. In: Renard KG, McElroy SA, Gburek WJ, Canfield HE, Scott RL, Eds. First interagency conference on research in the watersheds. US Department of Agriculture, Agricultural Research Service.

Huenneke LF, Vitousek PM. 1990. Seedling and clonal recruitment of the invasive tree *Psidium cattleianum*: implications for management of native Hawaiian forests. Biological Conservation 53:199–211.

IPCC. 2013. Working Group I Contribution to the IPCC fifth assessment report, climate change 2013: the physical science basis. Geneva: United Nations Environmental Program.

Jacobi JD, Warshauer FR. 1992. Distribution of six alien plant species in upland habitats on the Island of Hawai'i. In: Stone CP, Smith CW, Tunison JT, Eds. Alien plant invasions in native ecosystems of Hawai'i: management and research. Honolulu: University of Hawai'i. p 155–79.

Joe SM, Daehler CC. 2008. Invasive slugs as under-appreciated obstacles to rare plant restoration: evidence from the Hawaiian Islands. Biological Invasions 10:245–55.

Johnson AG. 2012. A water budget model and estimates of groundwater recharge for Guam. US Geological Survey. No. 2012-5028.

Juvik JO, Ekern PC. 1978. A climatology of mountain fog on Mauna Loa, Hawaii Island. Honolulu (HI): University of Hawaii.

Kagawa A, Sack L, Ke Duarte, James S. 2009. Hawaiian native forest conserves water relative to timber plantation: species and stand traits influence water use. Ecological Applications 19(6):1429–43.

Kim TS, Cai W, Jin F-F, Santoso A, Wu L, Guilyardi E, An S-I. 2014. Response of El Niño sea surface temperature variability to greenhouse warming. Nature Climate Change 8:786–90.

Knorr W, Prentice IC, House JI, Holland EA. 2005. Long-term sensitivity of soil carbon turnover to warming. Nature 433(7023):298–301.

Lau K-M, Wu H-T. 2011. Climatology and changes in tropical oceanic rainfall characteristics inferred from Tropical Rainfall Measuring Mission (TRMM) data (1998–2009). Journal of Geophysical Research: Atmospheres 116(D17):16.

Mair A, Fares A. 2010. Throughfall characteristics in three non-native Hawaiian forest stands. Agricultural and Forest Meteorology 150:1453–66.

McIntosh MD, Schmitz JA, Benbow ME, Burky AJ. 2008. Structural and functional changes of tropical riffle macroinvertebrate communities associated with stream flow withdrawal. River Research and Applications 24:1045–55.

Meehl GA. 1996. Vulnerability of freshwater resources to climate change in the tropical Pacific region. Water, Air, and Soil Pollution 92:203–13.

Milleham L, Taylor RG, Todd M, Tindimugaya C, Thompson J. 2009. The impact of climate change on groundwater recharge and runoff in a humid, equatorial catchment: sensitivity of projections to rainfall intensity. Hydrological Sciences Journal des Sciences Hydrologiques 54(4):727–38.

Milly PC, Dunne KA, Vecchia AV. 2005. Global pattern of trends in streamflow and water availability in a changing climate. Nature 438:347–50.

Milly PCD, Wetherald RT, Dunne KA, Delworth TL. 2002. Increasing risk of great floods in a changing climate. Nature 415:514–17.

Mimura N, Nurse L, McLean R, Agard J, Briguglio L, Lefale P, Payet R, Sem G. 2007. Small Islands. In: Parry ML, Canziani OF, Palutikof JP, van der Linden PJ, Hanson CE, Eds. Climate change 2007: impacts, adaptation, and vulnerability. Cambridge: Cambridge University Press. p 688–716.

Mitas CM, Clement A. 2005. Has the Hadley cell been strengthening in recent decades? Geophysical Research Letters 32:L03809.

Mudd RG, Giambelluca TW. 2006. Epiphyte water retention and evaporation in native and invaded tropical montane cloud forests in Hawai'i. In: Scholl MA, Ed. San Francisco (CA): American Geophysical Union.

Muller CJ, O'Gorman PA, Back LE. 2011. Intensification of precipitation extremes with warming in a cloud-resolving model. Journal of Climate 24:2784–800.

Nanko K, Giambelluca TW, Sutherland RA, Mudd RG, Nullet M, Ziegler AD. 2013. Erosion potential under *Miconia calvescens* stands on the Island of Hawai'i. Land Degradation & Development 26(3):218–26.

Olden JD, Poff NL. 2003. Redundancy and the choice of hydrologic indices for characterizing streamflow regimes. River Research and Applications 19:101–21.

Oliveira PJC, Davin EL, Levis S, Seneviratne SI. 2011. Vegetation-mediated impacts of trends in global radiation on land hydrology: a global sensitivity study. Global Change Biology 17:3453–67.

Ortega AR, Soraya de Almeida L, da Maia N, Angelo AC. 2006. Effect of shading on the growth of *Psidium cattleianum* Sabine seedlings in nursery conditions. CERNE 12(3):300–8.

Parker G, Wilcock PR, Paola C, Dietrich WE, Pitlick J. 2007. Physical basis for quasi-universal relations describing bankfull hydraulic geometry of single-thread gravel bed rivers. Journal of Geophysical Research: Earth Surface 112(F4):F04005.

Piao S, Ciais P, Huang Y, Shen Z, Peng S, Li J, Zhou L, Liu H, Ma Y, Ding Y et al. 2010. The impacts of climate change on water resources and agriculture in China. Nature 467:43–51.

Post DA, Jakeman AJ. 1999. Predicting the daily streamflow of ungauged catchments in S.E. Australia by regionalizing the parameters of a lumped conceptual rainfall-runoff model. Ecological Modelling 123:91–104.

Quan X-W, Diaz HF, Hoerling MP. 2004. Change in the tropical Hadley cell since 1950. In: Diaz HF, Bradley RS, Eds. The Hadley circulation: present, past, and future. Dordrecht: Kluwer Academics. p 85–120.

Risbey JS, Lewandowsky S, Langlais C, Monselesan DP, O'Kane TJ, Oreskes N. 2014. Well-established global surface warming in climate projections selected for ENSO phase. Nature Climate Change 4:834–40.

Roth KS, Dewald T. 1999. The National hydrography dataset. April 1, 1999 ed.: US Geological Survey, US Environmental Protection Agency.

Ruosteenoja K, Carter TR, Jylhä K, Tuomevirta H. 2003. Future climate in world regions: an intercomparision of model-based projections for the new IPCC emissions scenarios. Helsinki: Finnish Environment Institute. No. 644.

Safeeq M, Fares A. 2012. Interception losses in three non-native Hawaiian forest stands. Hydrological Processes 28(2):237–54.

Saxton KE, Rawls WJ. 2006. Soil water characteristic estimates by texture and organic matter for hydrologic solutions. Soil Science Society of America Journal 70:1569–78.

Scholl MA, Gingerich SB, Tribble GW. 2002. The influence of microclimates and fog on stable isotope signatures used in interpretation of regional hydrology: East Maui, Hawaii. Journal of Hydrology 264:170–84.

Smith LC, Turcotte DL, Isacks BL. 1998. Stream flow characterization and feature detection using a discrete wavelet transform. Hydrological Processes 12:233–49.

Stearns HT, Macdonald GA. 1946. Geology and ground-water resources of the Island of Hawaii. Honolulu (HI): Territory Government of Hawaii. pp 1–363.

Still CJ, Foster PN, Schneider SH. 1999. Simulating the effects of climate change on tropical montane cloud forests. Nature 398:608–10.

Strauch AM, Bruland GL, MacKenzie RA, Giardina CP. 2016. Soil and hydrological responses to wild pig (*Sus scofa*) exclusion from native and strawberry guava (*Psidium cattleianum*)-invaded tropical montane wet forests. Geoderma 279:53–60.

Strauch AM, MacKenzie RA, Bruland GL, Giardina CP. 2015. Climate driven changes to rainfall and streamflow patterns in a model tropical island hydrological system. Journal of Hydrology 523:160–9.

Takahashi M, Giambelluca TW, Mudd RG, DeLay JK, Nullet MA, Asner GP. 2011. Rainfall partitioning and cloud water interception in native forest and invaded forest in Hawai'i Volcanoes National Park. Hydrological Processes 25:448–64.

Timm O, Diaz HF. 2009. Synoptic-statistical approach to regional downscaling of IPCC twenty-first-century climate projections: seasonal rainfall over the Hawaiian Islands. Journal of Climate 22:4261–80.

Timm O, Diaz HF, Giambelluca TW, Takahashi M. 2011. Projection of changes in the frequency of heavy rain events over Hawai'i based on leading Pacific climate models. Journal of Geophysical Research 116:D04109.

Timm O, Takahashi M, Giambelluca TW, Diaz HF. 2013. On the relation between large-scale ciriculation pattern and heavy rain events over the Hawaiian Islands: Recent trends and future changes. Journal of Geophysical Research: Atmospheres 118:4129–41.

Timm OE, Giambelluca TW, Diaz HF. 2015. Statistical downscaling of rainfall changes in Hawai'i based on the CMIP5 global model projections. Journal of Geophysical Research: Atmosphers 120:92–112.

Tomlinson MS, De Carlo EH. 2003. The need for high resolution time series data to characterize Hawaiian streams. Journal of the American Water Resources Association 39:113–23.

Trenberth KE, Shea DJ. 2005. Relationships between precipitation and surface temperature. Geophysical Research Letters 32:L14703.

Uowolo AL, Denslow JS. 2008. Characteristics of the *Psidium cattleianum* (Myrtaceae) seed bank in Hawaiian lowland forests. Pacific Science 62(1):129–35.

USDA. 2008. Soil Survey geographic (SSURGO) database for Island of Hawaii Area, Hawaii. In: Service NRC, Ed. US Department of Agriculture.

USGS. 2005. National gap analysis program. In: Survey USG, Ed. Reston (VA).

VanShaar JR, Haddeland I, Lettenmaier DP. 2002. Effects of land-cover changes on the hydrological response of interior Columbia River basin forested catchments. Hydrological Processes 16:2499–520.

Waichler SR, Wemple BC, Wigmosta MS. 2005. Simulation of water balance and forest treatment effects at the H.J. Andrews Experimental Forest. Hydrological Processes 19(16):3177–99.

Westra S, Alexander LV, Zwiers FW. 2013. Global increasing trends in annual maximum daily precipitation. Journal of Climate 26:3904–18.

Wigmosta MS, Vail LW, Lettenmaier DP. 1994. A distributed hydrology-vegetation model for complex terrain. Water Resources Research 30:1665–79.

Wohl E, Barros A, Brunsell N, Chappell NA, Coe MT, Giambelluca TW, Goldsmith S, Harmon R, Hendrickx JMH, Juvik JO et al. 2012. The hydrology of the humid tropics. Nature Climate Change 2:655–62.

Yazaki K, Sano Y, Fujikawa S, Nakano T, Ishida A. 2010. Response to dehydration and irrigation in invasive and native saplings: osmotic adjustment versus leaf shedding. Tree Physiology 30:597–607.

Zhang W, An S, Xu Z, Cui J, Xu Q. 2011. The impact of vegetation and soil on runoff regulation in headwater streams on the east Qinghai-Tibet, China. Catena 87:182–9.

Zhou T, Zhang L, Li H. 2008. Changes in global land monsoon area and total rainfall accumulation of the last half century. Journal of Atmospheric Science 70:3–8.

Zimmerman N, Hughes RF, Cordell S, Hart P, Chang HK, Perez D, Like RK, Ostertag R. 2008. Patterns of primary succession of native and introduced plants in lowland wet forests in Eastern Hawai'i. Biotropica 40(3):277–84.